Adaptive Anisotropic Diffusion Method for Polarimetric SAR Speckle Filtering

Xiaoshuang Ma, Huanfeng Shen, *Senior Member, IEEE,* Liangpei Zhang, *Senior Member, IEEE,* Jie Yang, and Hongyan Zhang, *Member, IEEE*

***Abstract*—In this paper, we present an adaptive anisotropic diffusion (AD) method for the speckle filtering of polarimetric synthetic aperture radar (PolSAR) images. One of the main innovations of our work is that we employ a likelihood-ratio test method to measure the equality of two polarimetric covariance matrices to control the diffusivity, and thus consider the full polarimetric information and the statistical traits of PolSAR data in the diffusion process. Meanwhile, to overcome the drawback of the conventional AD methods, we integrate the local homogeneity information into the diffusion model to adaptively control the generosity of the filtering. Experiments were conducted on a simulated image and two airborne PolSAR images to illustrate the filtering performance, and the results show that the proposed method effectively reduces speckle, retains edges, and targets, and preserves the polarimetric scattering mechanisms.**

***Index Terms*—Anisotropic diffusion (AD), polarimetric synthetic aperture radar (PolSAR), speckle filtering.**

I. Introduction

SYNTHETIC aperture radar (SAR) systems have the capability to provide images of the earth in both day and night, and for almost all weather conditions. Polarimetric synthetic aperture radar (PolSAR) is an advanced form of SAR, which focuses on emitting and receiving fully polarized radar waves to characterize observed land targets. Compared with optical remote sensing data, PolSAR data have unique advantages in obtaining land-use and land-cover information. However, PolSAR data are inherently affected by speckle noise. The presence of speckle complicates the image interpretation and analysis, and reduces the effectiveness of target detection and classification [1]. Despeckling is, therefore, an essential procedure before using PolSAR images to obtain land information.

Speckle noise not only appears in the intensity image of each polarization, but also in the complex cross-product terms. It has been found that the diagonal terms of the polarimetric covariance matrix can be characterized by a multiplicative noise model, while the off-diagonal terms have the characteristics of a combined multiplicative and additive noise model [2]. This all makes the speckle reduction problem more complicated for PolSAR data than for single-polarization SAR data. In 1993, Novak and Burl [3] derived the polarimetric whitening filter (PWF) by optimally combining all the elements of the covariance matrix to reduce the speckle of amplitude images, and the off-diagonal terms of the covariance matrix were not filtered in the PWF filter. Lee *et al.* [4] proposed another algorithm to produce speckle reduced amplitude images, by using a multiplicative noise model and minimizing the mean square error. Goze *et al.* [5] generalized this filter to include all the terms of the covariance matrix. However, all of these filters introduced cross talk between polarization channels and did not well preserve the polarimetric properties [6].

To solve the above problems that the early algorithms encountered, Lee has done some remarkable researches on PolSAR speckle reduction [1], [8], [10]. In 1999, Lee developed the edge-aligned window technique and expanded his linear minimum mean-squared error (LMMSE) estimator in [7] to filter PolSAR data [1]. Lee's method was termed the refined Lee PolSAR filter. The refined Lee filter opened an important branch of filtering methods based on the LMMSE estimator. In [8], a novel method was proposed by Lee *et al.* to select neighboring pixels based on the same polarimetric scattering characteristics, and the selected pixels were used to filter the processed pixel by the LMMSE estimator. In [9], the pixels in the LMMSE estimator were selected by a technique of region growing, which is based on the intensity similarity of the polarimetric coherency matrices. Other LMMSE-based methods can be found in [10] and [11]. In addition to the methods based on LMMSE, some other filtering theories which were first developed for digital image denoising have also been extended to PolSAR image despeckling, including methods based on simulated annealing [12], nonlocal-means [13], and bilateral filtering [14].

Nonlinear anisotropic diffusion (AD) is a partial differential equation (PDE)-based filtering technique, which was the first proposed by Perona and Malik (PM model) in 1987 [16]. This method can effectively reduce the image noise and can simultaneously enhance important image features such as edges. In the last decade, the theory of AD has been widely extended to the filtering of SAR intensity images [17], [18]. However, to date, studies on PolSAR image despeckling by AD are lacking. To investigate the effectiveness of AD in filtering PolSAR data, we present a new AD-based filter for PolSAR image despeckling. It should be noted that, after the development of our algorithm, we became aware of an independent work studied by Sun *et al.* [15]

Manuscript received July 16, 2013; accepted May 27, 2014. Date of publication July 08, 2014; date of current version March 27, 2015. This work was supported in part by the National High Technology Research and Development Program (863) under Grant 2011AA120404, and in part by Wuhan Science and Technology Program under Grant 2013072304010825.

X. Ma and H. Shen are with the Department of Resource and Environmental Sciences, Wuhan University, 430079 Wuhan, China (e-mail: mxs.88@whu.edu.cn; shenhf@whu.edu.cn).

L. Zhang, J. Yang, and H. Zhang are with the State Key Laboratory of Information Engineering in Surveying, Mapping and Remote Sensing, Wuhan University, 430079 Wuhan, China (e-mail: zlp62@lmars.whu.edu.cn; yangjie@lmars.whu.edu.cn; zhanghongyan@whu.edu.cn).

Color versions of one or more of the figures in this paper are available online at http://ieeexplore.ieee.org.

Digital Object Identifier 10.1109/JSTARS.2014.2328332

that focuses on PolSAR speckle reduction via AD. However, our proposed method differs from the method in [15] in several important points. 1) First and foremost, differing from the method presented in [15], which only utilizes the intensity information to control the diffusivity and does not effectively take into account the statistical property of the speckle, the proposed method employs a likelihood-ratio test statistic to measure the equality of two polarimetric covariance matrices to calculate the diffusion coefficients, and thus considers the full polarimetric information and the statistical traits of the PolSAR data in the diffusion process. 2) In this research, we utilize the traits of the multiplicative speckle noise to obtain a local homogeneity index (LHI), and we use this to adaptively control the generosity of the diffusion, with the aim being to prevent the smearing of fuzzy structures that occurs in the conventional diffusion-based method. 3) Compared with the method of Sun *et al.* [15], which has several parameters that need to be chosen, the diffusion time is the only parameter that needs to be tuned in the proposed AD model, which ensures the algorithm's efficiency and practicality.

The remainder of this paper is organized as follows. In Section II, we describe the basic principles of filtering PolSAR data. In Section III, the properties of nonlinear AD are analyzed, and the proposed filtering method is presented. The filtering results for a simulated image and two real PolSAR images are then reported in Section IV. Finally, the conclusion is drawn in Section V.

II. Filtering Principles of PolSAR Data

Polarimetric radar measures the complex scattering matrix of a medium with quad polarizations. Single-look PolSAR data are characterized by the scattering matrix

$$S = \begin{bmatrix} S_{HH} & S_{HV} \\ S_{VH} & S_{VV} \end{bmatrix} \tag{1}$$

where S_{HV} is the scattering element of horizontal transmitting and vertical receiving polarization with the combination of the amplitude $|S_{HV}|$ and the phase ϕ_{HV} : $S_{HV} = |S_{HV}|e^{i\phi_{HV}}$, and the other elements are similarly defined. For the reciprocal backscattering case, $S_{HV} = S_{VH}$. The backscattered radar signal from each resolution cell is characterized by the tridimensional target vector $X = (S_{HH}, \sqrt{2}S_{HV}, S_{VV})^T$, where T is the transposition operator. The span (or total power) is $span = |S_{HH}|^2 + 2|S_{HV}|^2 + |S_{VV}|^2$. Single-look polarimetric data can also be represented by a polarimetric covariance matrix, which is generated from the outer product of the associated target vector X with its conjugate transpose X^H, as shown at the bottom of the page.

SAR data are frequently multilook processed for speckle reduction and data compression by averaging several neighboring one-look pixels as shown at the bottom of the page, where the superscript * denotes the complex conjugate and L denotes the number of looks. The polarimetric covariance matrix is a 3×3 Hermitian positive definite matrix. It has been found that, for fully developed speckle, the L-look covariance matrix C_z follows a complex Wishart distribution [19]

$$p\Big(C_z|\sum\Big) = \frac{|C_z|^{L-3}\exp\{-Ltr\sum^{-1}C_z\}}{Q(L)|\sum|^L} \tag{4}$$

with

$$Q(L) = \frac{\pi^3\Gamma(L)\Gamma(L-1)\Gamma(L-2)}{L^{3L}} \tag{5}$$

where $tr(\cdot)$ and $|\cdot|$ are, respectively, the trace and the determinant operators, and $\sum$ denotes the population covariance matrix.

The PolSAR speckle noise model is quite complicated. It is well known that the intensity (i.e., the diagonal elements of the polarimetric covariance matrix C) can be characterized by a multiplicative noise model [20]. An important trait of this multiplicative noise is that the ratio of the intensity's standard deviation to the mean [or coefficient of variation (CV)] is a constant for a given number of looks

$$CV = \sqrt{\frac{1}{L}} \tag{6}$$

where L is the number of looks. In 2003, López-Martínez and Fabregas [2] found that the off-diagonal terms of C are influenced by multiplicative noise and two different additive noise terms. After determining this model of PolSAR speckle noise, López-Martínez proposed an algorithm that filters each off-diagonal term separately from the diagonal terms, based on the off-diagonal term model [21]. Lee *et al.* [1], however, argued that filtering the off-diagonal terms separately could introduce artifacts, and that some of the early algorithms, which exploit the statistical correlations between the HH, HV, and VV polarizations, could introduce crosstalk between the polarization channels. They suggested that several basic principles should be followed when filtering PolSAR data [1], which have since been widely adopted by scholars: 1) to avoid crosstalk between the

$$C = XX^H = \begin{bmatrix} |S_{HH}|^2 & \sqrt{2}|S_{HH}||S_{HV}|e^{(\phi_{HH}-\phi_{HV})i} & |S_{HH}||S_{VV}|e^{(\phi_{HH}-\phi_{VV})i} \\ \sqrt{2}|S_{HH}||S_{HV}|e^{(\phi_{HV}-\phi_{HH})i} & 2|S_{HV}|^2 & \sqrt{2}|S_{VV}||S_{HV}|e^{(\phi_{HV}-\phi_{VV})i} \\ |S_{HH}||S_{VV}|e^{(\phi_{VV}-\phi_{HH})i} & \sqrt{2}|S_{VV}||S_{HV}|e^{(\phi_{VV}-\phi_{HV})i} & |S_{VV}|^2 \end{bmatrix}. \tag{2}$$

$$C_z = \frac{1}{L}\sum_{i=1}^{L} C(i) = \begin{bmatrix} \left\langle |S_{HH}|^2 \right\rangle & \left\langle \sqrt{2}S_{HH}S_{HV}^* \right\rangle & \left\langle S_{HH}S_{VV}^* \right\rangle \\ \left\langle \sqrt{2}S_{HV}S_{HH}^* \right\rangle & \left\langle 2|S_{HV}|^2 \right\rangle & \left\langle \sqrt{2}S_{HV}S_{VV}^* \right\rangle \\ \left\langle S_{VV}S_{HH}^* \right\rangle & \left\langle \sqrt{2}S_{VV}S_{HV}^* \right\rangle & \left\langle |S_{VV}|^2 \right\rangle \end{bmatrix} \tag{3}$$

polarization channels, each element of the covariance matrix C should be filtered independently; and 2) to preserve the polarimetric properties, each term of C should be filtered in a manner similar to multilook processing by averaging the covariance matrices of neighboring pixels, i.e., all the terms of the covariance matrix should be filtered by the same amount (or filtered equally).

III. Proposed Adaptive Anisotropic Diffusive Filter for PolSAR Data

A. PM Model of AD

The basic idea behind AD, as proposed by Perona and Malik [16], is to evolve from an original image $u_0(x, y)$, which is defined in a convex domain $\Omega \subset R \times R$. A family of increasingly smooth images $u(x, y, t)$ is then derived from the solution of the following PDE:

$$\begin{cases} \frac{du}{dt} = div[G(|\nabla u|) \cdot \nabla u] \\ u(x, y, 0) = u_0(x, y) \end{cases} \tag{7}$$

where ∇ is the gradient operator, div is the divergence operator, and $|\cdot|$ denotes the magnitude. $G(\cdot)$ is the diffusion coefficient. A four-neighborhood discrete form of (7) is given by

$$u(x, y, t + \Delta t) = u(x, y, t) + \frac{\Delta t}{4} \sum_{p \in Z} G(\nabla u(p, t)) \cdot \nabla u(p, t) \tag{8}$$

where Z is the set of the four neighborhoods of pixel (x, y), p denotes a neighborhood of (x, y), and $\nabla u(p, t) = u(p, t) - u(x, y, t)$ is the image gradient at current time t. The above equation is recursive over time until it meets the stopping criterion. Perona and Malik suggested that a desirable diffusion coefficient should satisfy the basic condition that it diffuses more in smooth areas and less around high-intensity transitions, so that noise or unwanted texture are smoothed, while edges are sharpened. They put forward two such diffusion coefficients

$$G(X) = \frac{1}{1 + \left(\frac{X}{k}\right)^2} \tag{9}$$

and

$$G(X) = \exp\left(-\left(\frac{X}{k}\right)^2\right) \tag{10}$$

where k is an edge magnitude parameter. In most of the conventional AD methods, k is obtained by the "noise estimator" suggested by Canny [22]: at each iteration, a histogram of the absolute values of the gradient throughout the image is computed, and k is set to be equal to the 90% value of its integral. It has been found that there are no significant differences in the filtering results when using these two different diffusion coefficients. In this paper, we use the diffusion coefficient of (10) for all the applications.

We define G as the diffusion coefficient and $|d|$ as the absolute value of the gradient, and the relationship between them is plotted in Fig. 1. The basic properties of AD are formulated as follows.

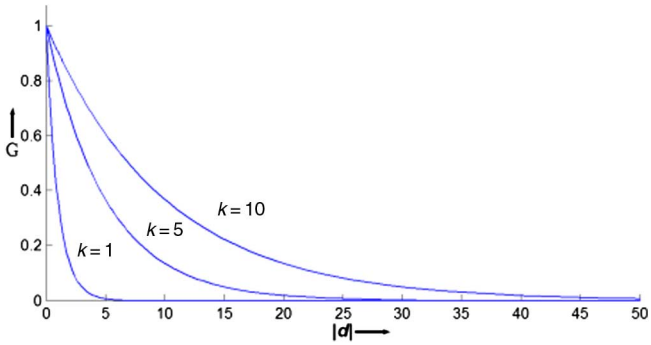

Fig. 1. Relationship between the diffusion coefficient and the absolute value of the gradient.

1) The range of G is [0, 1]. For any given parameter k, G monotonically decreases with $|d|$. If $|d| \to 0$, then $G \to 1$, which is isotropic diffusion (Gaussian filtering); if $|d| \to +\infty$, $G \to 0$, the diffusion flow is arrested and the edges are preserved.
2) For any given $|d|$, G monotonically increases with parameter k, which means that k controls the generosity of the anisotropic diffusive filter. For a higher value of k, the diffusion process is more likely to smooth the image and reduce the noise; while for a lower value of k, the diffusion process is more restricted and is more likely to preserve image features.

B. Proposed Adaptive PolSAR AD Model

Based on the aforementioned PolSAR filtering principles and the discrete scheme of the PM model, the proposed AD model for PolSAR filtering is formulated as follows:

$$C(x, y, t + \Delta t) = C(x, y, t) + \frac{\Delta t}{4} \sum_{p \in Z} F(\nabla C(p, t)) \times [C(p, t) - C(x, y, t)] \tag{11}$$

where $C(x, y)$ denotes the polarimetric covariance matrix of pixel (x, y), Z is the set of the four neighborhoods of pixel (x, y), $\nabla C(p, t)$ denotes the PolSAR image gradient, and the same diffusion coefficient $F(\nabla C(p, t))$ is used to filter each term of C independently and equally.

1) Calculation of the PolSAR Image Gradients: Two important issues should be concerned when applying the PM model to PolSAR despeckling. The first issue is the aforementioned PolSAR filtering principle. On the basis of this principle, the other issue is how to define the PolSAR image gradients and obtain robust and precise diffusion coefficients. In [15], Sun *et al.* only utilized the total intensity information to calculate the diffusion coefficients and to control the diffusivity, which is defined by us as "intensity-driven AD" (IDAD) in this paper. The shortcoming of this method, however, is that it could lead to two problems.

1) Polarimetric radar systems not only receive the amplitude of the backscattered waves but also receive the phase information of each polarization, which are both useful

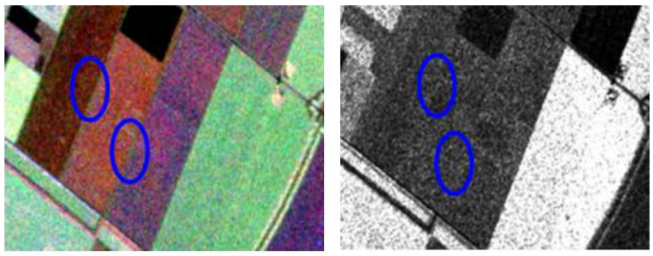

Fig. 2. Example showing the problem with IDAD. (a) Pauli RGB image of a PolSAR data set. (b) The span image of (a).

to discriminate land objects. If only the amplitude or intensity is used to control the diffusion process, the boundaries between different classes of object might be blurred, especially for those objects which have similar intensity information but have quite different phase information. To visualize this problem, we list a simple example in Fig. 2. As can be seen, in the Pauli RGB image, the edges and boundaries are quite visible between two classes of objects in the blue ellipses, which implies that these objects have totally different polarimetric information; while in the span image, these objects are very similar in intensity (low-intensity gradients on the boundaries). In such a case, if only the intensity gradients are used, diffusion could take place on their boundaries, and the edges might be blurred. How to use the full polarimetric information in the calculation of the gradients is, therefore, an important issue when applying AD to filter PolSAR images.

2) PM algorithm was first developed in the additive white Gaussian noise (AWGN) hypothesis. In the AWGN setting, a smaller Euclidean distance corresponds to a higher likelihood that the two signal pixels (without noise) are equal. Nevertheless, for SAR intensity image, which is affected by speckle noise (follows a negative exponential distribution), the simple Euclidean distance loses its significance, and one needs a different similarity measure in order to keep identifying the signal pixels that are more likely to be equal to the reference one. However, the simple Euclidean distance is used in [15] to calculate the gradients in the intensity image, and then the diffusion coefficients are derived from it, which might not be appropriate.

It is, therefore, important to take into account the full polarimetric information and the statistical property of the PolSAR data in the diffusion process when applying the PM algorithm to PolSAR filtering. In this research, we deploy a likelihood-ratio test method to measure the equality of two covariance matrices, and regard this equality between a pixel and its neighborhood as the PolSAR image gradient. This likelihood-ratio test method was first proposed by Conradsen *et al.* [23]. We assume that the independent 3×3 Hermitian positive definite matrices (covariance matrices) X and Y are complex Wishart distributed, i.e., $X \in W_c(3, n, \sum_x)$ with $\hat{\sum}_x = 1/nX$ and $Y \in W_c(3, m, \sum_y)$ with $\hat{\sum}_y = 1/mY$, where $m = n$, which is the number of looks. Then, their sum also follows a complex Wishart distribution: $S = X + Y \in W_c(3, n+m, \sum)$, with $\hat{\sum} = 1/(m+n)(X+Y)$. Consider the null hypothesis H_0: $\sum_x = \sum_y$, which states that the two matrices are equal, against the alternative hypothesis H_1: $\sum_x \neq \sum_y$.

If H_0 is true, the likelihood-ratio test statistic can be derived as

$$Q = \frac{(n+m)^{3(n+m)}}{n^{3n}m^{3m}} \frac{|X|^m |Y|^n}{|X+Y|^{m+n}}. \tag{12}$$

The logarithm of the likelihood-ratio test statistic is

$$\ln Q = n(6\ln 2 + \ln|X| + \ln|Y| - 2\ln|X+Y|). \tag{13}$$

Since all the pixels in the same image have the same number of looks n, the above equality measurement can be simplified as

$$\ln Q = (6\ln 2 + \ln|X| + \ln|Y| - 2\ln|X+Y|). \tag{14}$$

In this paper, we regard the $\ln Q$ between two neighboring pixels as the image gradient. Details of the aforementioned derivation can be found in [23] and [13]. It can be verified that $\ln Q = 0$ when the two complex Wishart distributions are the same; otherwise, $\ln Q < 0$. $\ln Q$ satisfies the basic condition of constructing the diffusion coefficient G in (10): G monotonically decreases with $|\ln Q|$. In homogeneous areas with polarimetric and physically similar pixels (follow a similar complex Wishart distribution), the likelihood-ratios $\ln Q$ between pixels are close to zero and the diffusion coefficients are close to one, which is isotropic diffusion (Gaussian filtering). In such a case, the speckle is reduced; otherwise, the diffusion flow is arrested, and the edges and features are preserved. Since $\ln Q$ is obtained by the likelihood-ratio test between two covariance matrices, and it is based on the complex Wishart distribution, the full polarimetric information, and statistical traits of the PolSAR data are utilized in the diffusion process, rather than simply using the intensity information.

2) Adaptive PolSAR AD by the Integration of Local Homogeneity Information: Once the image gradient $\ln Q$ is obtained, the PolSAR PM AD model can be derived as

$$C(x,y,t+\Delta t) = C(x,y,t) + \frac{\Delta t}{4} \sum_{p \in Z} G(\ln Q(p,t)) \cdot [C(p,t) - C(x,y,t)]. \tag{15}$$

The PM AD model has shown outstanding filtering performances, and there have been extensive researches into how to improve this method further. One perspective is that the conventional AD methods are gradient-dependent: the degree of diffusive smoothing in these methods is controlled by the image gradient information, and an alternative method for determining the significant information in an image may be to consider the local region homogeneity. Integrating this kind of local information into the AD model could improve its performance. In [24], Parker and Schnable suggested multiplying the diffusion coefficient by a local heterogeneity index, called approximate entropy. Other methods that use a measure of local information to control the diffusion can be found in [25] and [26].

Furthermore, some other researchers have argued that a troubling property of AD is its implicit use of a unique threshold on the luminance gradient [i.e., the edge magnitude parameter k

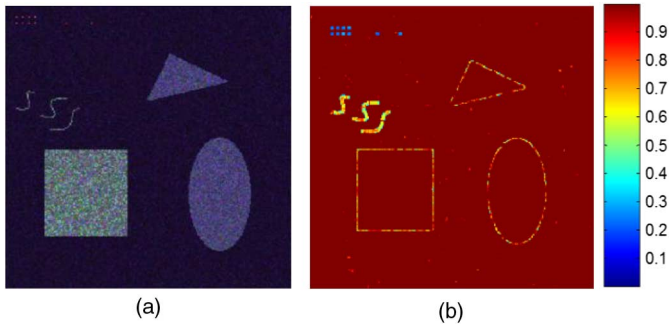

Fig. 3. Experiment to show the effectiveness of LHI in depicting local homogeneity. (a) The simulated image. (b) The corresponding LHI map.

in (10)] [27]. As pointed out by Saha and Udupa [28], the PM AD model is a very useful approach, an important drawback of this method, however, is that it does not use any morphological or structural information to control the extent of the diffusion in different regions. In the original AD method, the flow across object boundaries is reduced due to the high image gradients at boundaries. However, the image gradients on fuzzy boundaries are often not high enough to arrest the flow. As a result, fine structures and boundaries are often blurred after filtering. As mentioned before, the parameter k in the diffusion coefficient controls the generosity of the anisotropic diffusive smoothing. When k is large, the generosity of filtering is high, and the noise can be reduced, but it would be more likely to blur edges. On the other hand, when k is small, the generosity of filtering is low, and the edges can be preserved, but more noise would survive after filtering. In the conventional AD methods, k is fixed for each region in an iteration, and adaptive control of k is lacking. Saha and Udupa [28] suggested that taking a fine control of k to adaptively determine the generosity of diffusion for each region could alleviate the problem of blurring fine edges. They argued that it is better to use a restricted parameter for filtering in heterogeneous regions (structures and the vicinity of boundaries) and to use a generous filtering parameter in homogeneous regions.

Inspired by the above researches, to improve our PolSAR AD method, we also employ a strategy to integrate the local homogeneity information into the diffusion model, and to adaptively control the generosity of the filtering. As we stressed before, an important trait of the multiplicative noise of SAR images is that the intensity's coefficient of variation in homogeneous areas is close to a constant, for a given number of looks. Therefore, we can utilize this trait to obtain the local homogeneity information of a pixel. In this paper, we define the LHI as

$$LHI(x,y) = \frac{CV}{cv(x,y)} \tag{16}$$

where CV is the intensity's coefficient of variation in homogeneous areas, as obtained by (6), $cv(x,y)$ is the coefficient of variation of a pixel's 3×3 neighboring window, and the LHI values are obtained in the original speckled image (before evolving the image). The range of LHI is [0, 1] (some values in homogeneous areas might be upon 1, and we set them to 1 to ensure the stability of our model). For pixels located in homogeneous areas, their LHI values will be close to 1; while for

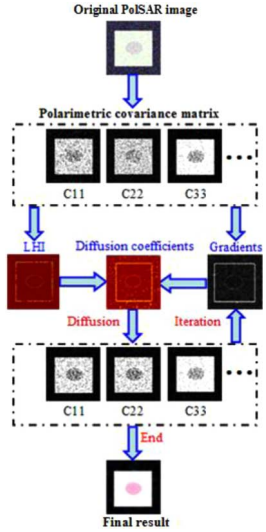

Fig. 4. Framework of the proposed adaptive PolSAR AD method.

edges or pixels located in the vicinity of boundaries, their LHI values are much lower than 1. To visualize the effectiveness of LHI in depicting local homogeneity, we present the LHI map of a four-look simulated image (Fig. 3). This simulated image was generated by the method proposed in [29]. As we can see, the edges, boundaries, and point targets are all successfully "detected" in the LHI map.

Once the LHI values are obtained before the evolution, we can then replace the parameter k at each iteration (often estimated by the Canny "noise estimator") with a local homogeneity controlled parameter k_σ

$$k_\sigma(x,y,t) = k(t) \cdot LHI(x,y). \tag{17}$$

By doing so, the proposed method is able to affect a restricted diffusion around edges and in the vicinity of boundaries, and allows a generous diffusion in the interior of homogeneous regions. Finally, a four-neighborhood discrete form of the adaptive PolSAR AD (APAD) model is given by

$$\begin{aligned} &C(x,y,t+\Delta t) \\ &\quad = C(x,y,t) + \frac{\Delta t}{4} \sum_{p \in Z} \exp\left(-\left(\frac{\ln Q(p,t)}{k(t) \cdot LHI(x,y)}\right)^2\right) \\ &\qquad \times [C(p,t) - C(x,y,t)] \end{aligned} \tag{18}$$

where $C(x,y,t)$ denotes the covariance matrix of pixel (x,y) at time t, Z is the set of the neighborhoods of pixel (x,y), and $\ln Q(p,t)$ is the equality between pixel (x,y) and its neighborhood (i.e., the PolSAR image gradient of pixel (x,y)). To conclude the proposed method, we summarize its steps by Fig. 4. First, initialize Δt as 0.05 and set the time T of the diffusion, and calculate the LHI values by (16). Then, in each iteration, calculate the gradients by the likelihood-ratio test statistic of (14) and obtain the parameter k by the Canny "noise estimator," and evolve the image by (18). Finally, output the filtering result if the iteration time is reached. In the proposed method, the total diffusion time T is the only parameter that needs to be tuned, which makes the method more applicable and efficient. In fact, we found that in most cases, the filtering results are quite

TABLE I
BASIC PARAMETERS OF THE REAL POLSAR DATA SETS

Data set	Platform	Polarization	Spatial resolution	Band
San Francisco	AIRSAR	Quad-polarization	10 m × 10 m	L-band
Haikou	XSAR	Quad-polarization	1 m × 1 m	X-band

effective when T is set as 20. Of course, in practice, we still need to test if a larger value of T can improve the results. Furthermore, to avoid over-smoothing and unnecessary computation, we also deploy another stopping criterion: the diffusion is stopped automatically when the residual error, defined as the mean square error of the span images between two iterations, is less than a threshold Tr (Tr is set as 0.01 dB in our method).

IV. EXPERIMENTAL RESULTS OF POLSAR SPECKLE FILTERING

In this section, to investigate the filtering performance of the APAD filter presented in Section III, the results obtained with a simulated PolSAR image and two real PolSAR images (Table I) are reported. Two filters are also implemented for comparison purposes: the IDAD filter proposed by Sun *et al.* [15] and the refined Lee filter [1].

A. Experiments With a Simulated PolSAR Image

An experiment was conducted on a four-look simulated PolSAR image to assess the performance of speckle reduction. First, to illustrate the effect of integrating the LHI into our method, we present the filtering results of the proposed PolSAR AD with and without the LHI. As can be seen in Fig. 5(f) and (g), on the one hand, the speckle reduction in the images filtered by both methods is quite similar. This is because, in homogeneous areas, the LHI values are close to 1, and thus $k_\sigma \approx k$, and the two methods have similar generosity of filtering. On the other hand, some edges and point targets are smeared if LHI is not considered. However, the proposed APAD method does not encounter the above problem because we use the local homogeneity information to affect a restricted diffusion around the edges and point targets.

Fig. 5 also shows the filtering results of the refined Lee filter and IDAD filter. As can be observed in Fig. 5(d), the refined Lee filter shows a positive filtering performance: the speckle is reduced to some degree, and the edges and point signatures are preserved. Compare with the refined Lee filter, IDAD shows a much better speckle reduction performance [Fig. 5(e)], but the boundaries of the triangle and the ellipse are slightly blurred. The reason for this problem might be that the gradients of intensity between these two objects and the background are quite low [Fig. 5(c)], and diffusion has taken place on the boundaries since only intensity is taken into account. However, it should be noted that IDAD shows a better performance in retaining the isolated point targets than the PolSAR AD without considering LHI [Fig. 5(f)]. This may be because that the presence of noise, especially when the gradient generated by noise is comparable to that by image features, might drive the diffusion process to undesirable results [16], [30]. In IDAD, a Gaussian smoothing operation is implemented on the span image before each iteration

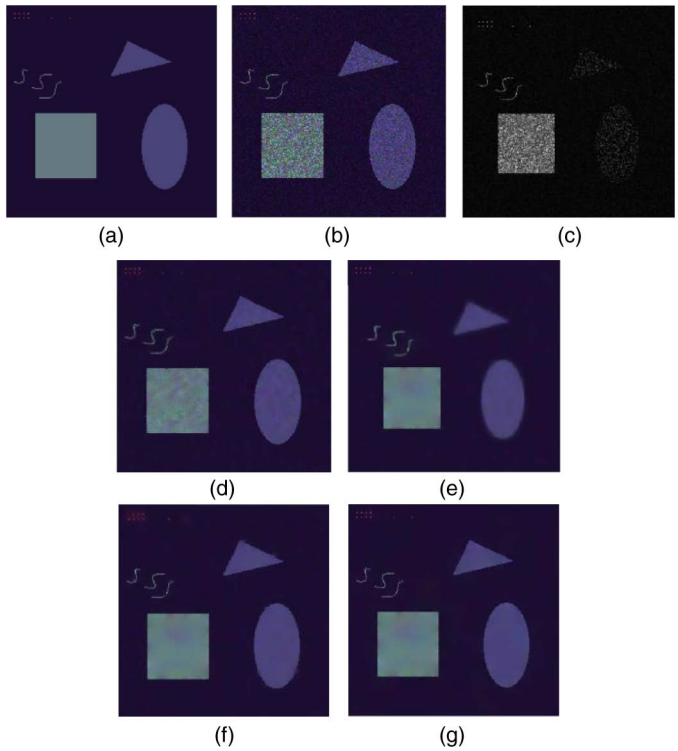

Fig. 5. Comparison of the filtering performances with a simulated image. (a) Pauli RGB image of the noise-free data. (b) Four-look speckled image. (c) Span image of (b). (d) The refined Lee filter shows a positive performance in reducing speckle and retaining edges. (e) IDAD shows an outstanding performance in speckle reduction, but the boundaries of the triangle and the ellipse are slightly blurred. (f) Filtering results of PolSAR AD without considering LHI. (g) The filtering results of adaptive PolSAR AD.

[15], which alleviates the above problem to some degree and leads to the better preservation of point targets than for PolSAR AD without LHI. Compared with the refined Lee filter and IDAD, the filtering result of the proposed APAD is desirable [Fig. 5(j)]: the speckle noise is effectively reduced, and the edges and point targets are effectively preserved.

In order to objectively assess the effectiveness of the speckle suppression of each method, three quantitative indices are introduced: the peak signal-to-noise ratio (PSNR), the equivalent number of looks (ENL) and the structural similarity (SSIM) index. PSNR is a metric that measures the quality of a processed image, compared with the noise-free image. A high value of PSNR represents a high image quality; ENL is an indicator that is widely used to indicate the speckle noise level of SAR images. A high value of ENL represents a low level of speckle noise; A high SSIM value indicates better preservation of the edges and details. All three of these indices are calculated in the span image. This is because the span image is a weighted average of the HH, HV, and VV intensities, and many features that may appear differently in each polarization channel will show up in the span image. One can observe in Table II that IDAD and APAD are much more efficient than the refined Lee filter in speckle reduction. For the PSNR and the SSIM, APAD shows the best filtering performance among the three methods. For the ENL, IDAD gets a slightly higher value than APAD, which is because the image filtered by IDAD is somewhat over smoothed.

TABLE II
PSNR AND ENL OF THE IMAGES FILTERED BY THE DIFFERENT METHODS

		Refined Lee	IDAD	APAD
Simulated image	PSNR (dB)	70.1	81.3	**84.4**
	ENL	28.4	**51.7**	50.9
	SSIM	0.883	0.902	**0.939**
San Francisco	ENL	30.8	39.5	**43.6**
Haikou	ENL	32.0	45.4	**46.3**

B. Experiments With Two Real PolSAR Images

Compared with simulated images, real PolSAR images have much more complicated scenes, and they are often used to inspect the filtering performance of retaining edges and preserving polarimetric scattering mechanisms. It has been recognized that the polarimetric scattering mechanisms are quite useful in land-use classification and scene interpretation, and a good PolSAR speckle filtering method should possess the trait of preserving this important polarimetric information. In the last two decades, "target decomposition theorems" have been widely investigated to depict the scattering mechanisms of SAR signals. Among them, the Freeman and Durden decomposition [31] and the H/A/alpha decomposition [32] are two of the most important theorems.

1) Experiments With the San Francisco Data Set: The San Francisco data set was acquired by the AIRSAR project of the National Aeronautics and Space Administration/Jet Propulsion Laboratory, and was processed by the European Space Agency as a four-look data set. This data set has been widely used in the study of the polarimetric scattering mechanisms, and contains several classes of typical land objects that have different scattering mechanisms. In [31], Freeman and Durden developed a scattering model-based decomposition to characterize the dominant scattering mechanism of pixels. In this decomposition model, the scattering characteristics are decomposed into three basic scattering mechanisms: surface (or odd) scattering, double-bounce scattering, and volume scattering. The dominant scattering category of a pixel is determined by its highest power among the three scattering components. To illustrate the proposed method's ability to preserve the dominant scattering mechanism, Freeman and Durden decomposition was undertaken on a subset of the San Francisco image (501×421 pixels) filtered by the different methods (Fig. 6). The images are displayed using magnitudes of surface scattering (blue), double-bounce scattering (red), and volume scattering (green).

As can be seen, the image filtered by the refined Lee filter shows the problems of a scalloped appearance and a block effect [Fig. 6(b)], which is due to the use of the edge-aligned windows. Furthermore, many of the fine edges are not well retained in the refined Lee filtered image. Compared with the refined Lee filter, IDAD reveals better filtering traits in both speckle reduction and edge retaining. Both of the above two methods have, however, smeared some of the strong point signatures (for example, buildings in the forest area and ships on the sea), and have lost some detailed polarimetric information in the urban area. This is attributed to the fact that both the refined Lee filter and IDAD are the intensity-driven filters and they do not utilize the phase information: for the refined Lee filter, the homogeneous pixels

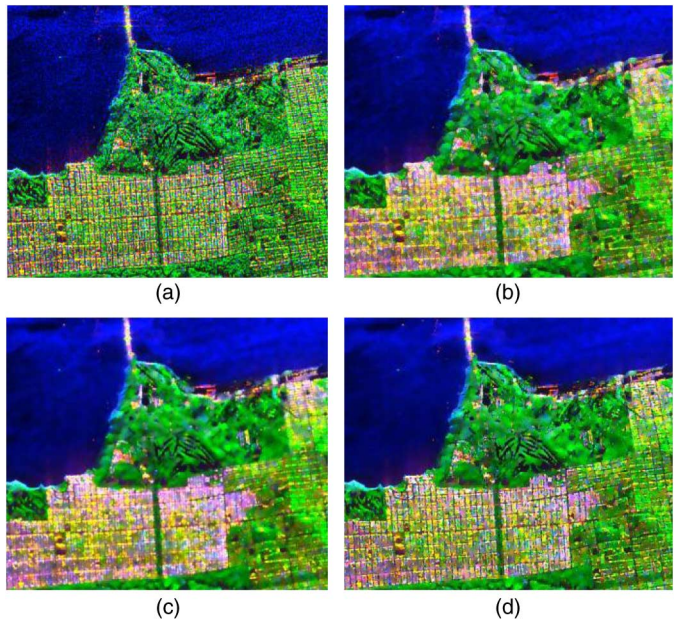

Fig. 6. Comparison of the filtering results with the San Francisco image. (a) Freeman RGB image of the original data. (b) The result of the refined Lee filter, which results in a block effect and blurred edges. (c) The result of IDAD shows a better filtering performance than the refined Lee filter. (d) The result of the proposed method effectively reduces speckle, preserves the dominant scattering properties, and retains the details.

are selected based on the edge-aligned window obtained in the span image; for IDAD, the gradients are calculated in the span image. The improvement in the APAD-filtered data is evident: the speckle noise is effectively reduced (Table II), the details and spatial resolution are retained, and the dominant scattering mechanism is well preserved [Fig. 6(d)].

The retention of strong returns from point targets is essential for target and man-made structure detection, and to preserve the original polarimetric signatures and properties of these targets is, therefore, important for some applications. In certain PolSAR filtering algorithms [8], [10], isolated point targets are detected and are kept unfiltered. Although, in the proposed method, no special strategies are deployed to detect and retain these targets, we undertook an experiment to show that the proposed method is able to preserve their original polarimetric properties. We chose three point target pixels in the filtered images, and we plot the magnitudes of their three basic scattering mechanisms in Fig. 7. Meanwhile, to quantitatively evaluate the preservation of point targets, we have also calculated the sum of the deviation (SD) of the magnitudes between a speckled pixel and a filtered pixel

$$SD = \sum_{i=1}^{3} \sqrt{(A_1{}^i - A_0{}^i)^2 + (B_1{}^i - B_0{}^i)^2 + (C_1{}^i - C_0{}^i)^2} \tag{19}$$

where the superscript i denotes pixel P1 to P3. A_0, B_0, and C_0 are the magnitudes of odd, double, and volume scattering of the original pixel, respectively; and A_1, B_1, and C_1 are the magnitudes of odd, double, and volume scattering of the filtered pixel, respectively. Here, it can be easily seen that, among the three methods, the magnitudes of the APAD-filtered point targets are mostly in line with their original states [Fig. 7(e)], which

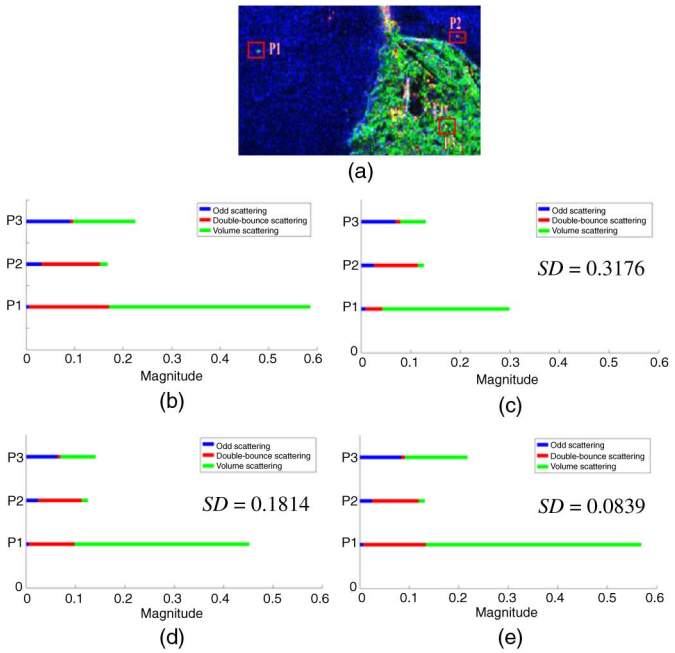

Fig. 7. Comparison of the preservation of point target signatures. (a) A subset of the San Francisco image with the selected point targets marked by red rectangles. (b)–(e) The magnitudes of the three basic scattering mechanisms of point targets in the original image and in the images filtered by the refined Lee filter, IDAD, and APAD, respectively.

confirms the proposed method's ability to preserve the original scattering mechanisms of point targets. Both the refined Lee filter and IDAD distort the scattering mechanisms of the point targets to some degree. For the refined Lee filtered data in particular, the dominant scattering category of P3, which was originally volume scattering, changes to odd scattering [Fig. 7(c)].

To further validate that the proposed method is able to preserve the scattering properties of point targets, we plot the polarimetric signatures of pixel P3 filtered by the different methods. The polarimetric signatures, introduced by Van Zyl [33], plot the normalized copolarization or cross-polarization power density σ when exploring all the polarization space, which can show the amount of power that will be received from a given scatterer for any polarization. Fig. 8 shows the copolarization polarimetric signatures of P3. As can be observed, a close agreement is reached between the signatures from the original pixel and the pixel filtered by APAD [Fig. 8(d)], while distinct disagreements arise for the pixels filtered by the refined Lee filter and IDAD. This experiment once again indicates the superiority of APAD in preserving the original polarimetric scattering signatures of point targets. Figs. 7 and 8 imply that APAD effectively arrests the diffusion around the strong point targets, thereby preserving their original polarimetric information. In contrast, both the refined Lee filter and IDAD result in the smearing of the point target signatures.

2) Experiments With Haikou Data Set: The second real image used for illustration is the Haikou image, which was obtained from a X-band airborne sensor. Fig. 9 shows the filtering results of the different methods on a subset of the Haikou image (751×301 pixels). As expected, the refined Lee filter shows a block effect and blurs the edges [Fig. 9(b)]. IDAD shows an improvement in speckle reduction (Table II) and edge

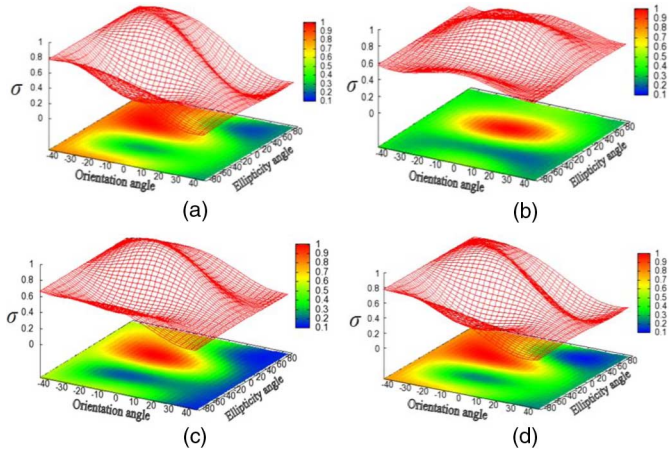

Fig. 8. Comparison of the copolarization signatures of a point target. (a) The original copolarization signatures of P3. (b)–(d) The copolarization signatures of P3 filtered by the refined Lee filter, IDAD, and APAD, respectively.

2) *Experiments with Haikou Data Set:*

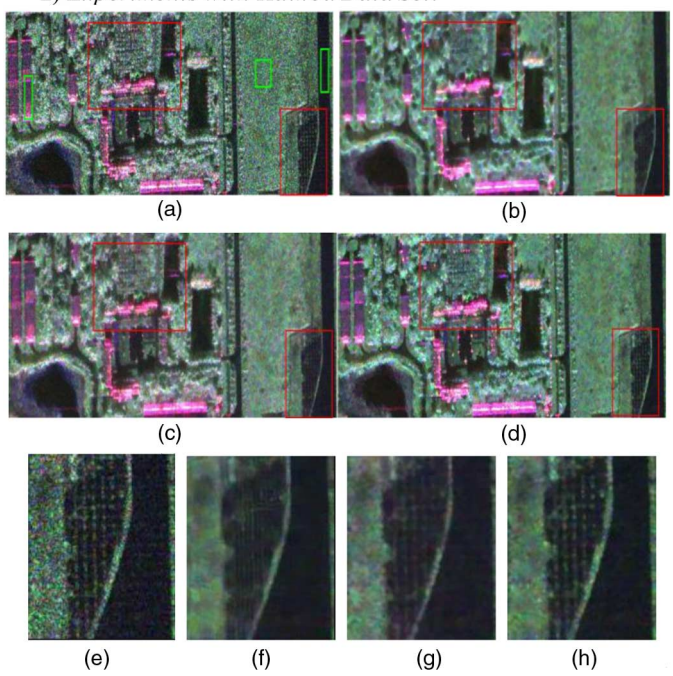

Fig. 9. Comparison of the filtering performances with the Haikou image. (a) Pauli RGB image of the original subset. (b)–(d) The filtering results of the refined Lee filter, IDAD, and APAD, respectively. (e)–(h) Detailed regions cropped from (a) to (d).

preservation, compared with the refined Lee filter (marked by red rectangles). The proposed method again shows its outstanding filtering traits of reducing speckle and retaining details, especially for the point targets [Fig. 9(d)].

H/A/alpha decomposition, which is based on an eigenvalue analysis of the polarimetric coherency matrix, was proposed by Cloude and Pottier [32]. In this decomposition model, the polarimetric scattering entropy (H) is an index used to describe the degree of statistical disorder of each distinct scatter type within the ensemble (i.e., the randomness of the scattering). The polarimetric scattering anisotropy (A) measures the relative importance of the second and the third eigenvalues of the eigen

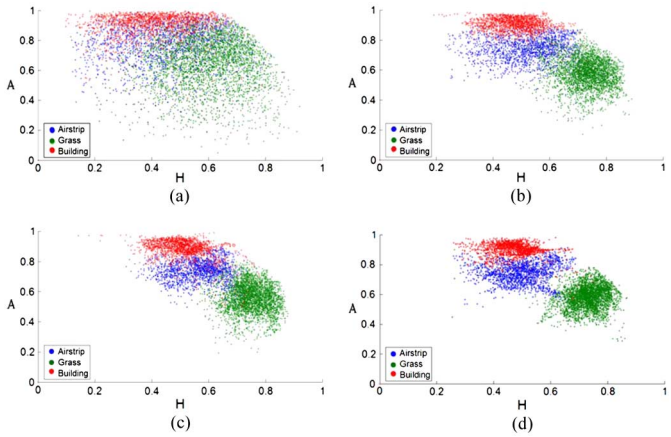

Fig. 10. Experiment to inspect the effect of filters on polarimetric scattering entropy and anisotropy. (a)–(d) The distribution of the entropy and anisotropy values for the original data and the data filtered by the refined Lee filter, IDAD, and APAD, respectively.

decomposition. Speckle filtering and other averaging processes can affect the inherent scattering characteristics of each pixel. The results of entropy and anisotropy, in particular, are dependent on the averaging process. As pointed out in [8], in general, the entropy value increases with the amount of averaging, but the anisotropy decreases.

To illustrate the effect of filters on H and A, we plot the scattergrams of the original and the filtered H and A values for three classes [marked by green rectangles in Fig. 9(a)]. We can see from Fig. 10 that H and A effectively describe the scattering mechanisms of each class: for the airstrip pixels, their dominant scattering mechanism is odd scattering and there are low amounts of the other scattering types, and hence they have low H values; for the grass pixels, the randomness of their scattering mechanisms is high, and hence they have high H values; for the building pixels, the backscattered signals mainly come from double-bounce scattering, and hence they have low H values. In addition, since their second most dominant scattering mechanisms (odd scattering) are of larger amounts than the third ones (volume scattering), the buildings have high A values. It can be observed that, generally speaking, the H values computed from the filtered images increase and the A values computed from the filtered images decrease. This is due to the averaging effect of the filters. Furthermore, we can see that the distributions of the H and A values are more concentrated and these four classes are more separable in the data filtered by IDAD and APAD, which verifies that the proposed method and IDAD perform better in speckle reduction and enhancing the class separation than the refined Lee filter.

V. Conclusion

In this paper, we propose an adaptive AD method for the speckle filtering of PolSAR images. A likelihood-ratio test method is used to calculate the diffusion coefficient, and an LHI is adopted to adaptively control the generosity of the diffusion. Experiments were conducted on a simulated image and two real PolSAR images, revealing the good filtering performance of the proposed method in reducing speckle, retaining edges and targets, and preserving the polarimetric scattering mechanisms. It must be pointed out that, to utilize the full polarimetric information in the AD model, we employ the likelihood-ratio test statistic to measure the equality of two covariance matrices. This test is based on the assumption that the covariance matrix follows a complex Wishart distribution, and it is only satisfied for areas with fully developed speckle. However, for those scenes with lots of details, such as urban areas in very high-resolution PolSAR images, the equality measures derived from the Wishart PDF might not be appropriate, and more complicated statistical models [34], [35] need to be considered. This is application and problem oriented.

References

[1] J. S. Lee, M. R. Grunes, and G. D. Grandi, "Polarimetric SAR speckle filtering and its implication for classification," *IEEE Trans. Geosci. Remote Sens.*, vol. 37, no. 5, pp. 2363–2373, Sep. 1999.

[2] C. López-Martínez and X. Fabregas, "Polarimetric SAR speckle noise model," *IEEE Trans. Geosci. Remote Sens.*, vol. 41, no. 10, pp. 2232–2242, Oct. 2003.

[3] L. M. Novak and M. C. Burl, "Optimal speckle reduction in polarimetric SAR imagery," *IEEE Trans. Aerosp. Electron. Syst.*, vol. 26, no. 2, pp. 293–305, Mar. 1990.

[4] J. S. Lee, M. R. Grunes, and S. A. Mango, "Speckle reduction in multipolarization, multifrequency SAR imagery," *IEEE Trans. Geosci. Remote Sens.*, vol. 29, no. 4, pp. 535–544, Jul. 1991.

[5] S. Goze and A. Lopes, "A MMSE speckle filter for full resolution SAR polarimetric data," *J. Electromagn. Waves Appl.*, vol. 7, no. 5, pp. 717–737, 1993.

[6] J. S. Lee and E. Pottier, *Polarimetric Radar Imaging: From Basics to Applications*. Boca Raton, FL, USA: CRC Press, 2009.

[7] J. S. Lee, "Digital image enhancement and noise filtering by use of local statistics," *IEEE Trans. Pattern Anal. Mach. Intell.*, vol. PAMI-2, no. 2, pp. 165–168, Mar. 1980.

[8] J. S. Lee, M. R. Grunes, D. L. Schuler, E. Pottier, and L. F. Famil, "Scattering-model-based speckle filtering of polarimetric SAR data," *IEEE Trans. Geosci. Remote Sens.*, vol. 44, no. 1, pp. 176–187, Jan. 2006.

[9] G. Vasile, E. Trouve, J. S. Lee, and V. Buzuloiu, "Intensity-driven adaptive-neighborhood technique for polarimetric and interferometric SAR parameters estimation," *IEEE Trans. Geosci. Remote Sens.*, vol. 44, no. 6, pp. 1609–1621, Jun. 2006.

[10] J. S. Lee, J. H. Wen, T. L. Ainsworth, K. S. Chen, and A. J. Chen, "Improved sigma filter for speckle filtering of SAR imagery," *IEEE Trans. Geosci. Remote Sens.*, vol. 47, no. 1, pp. 202–213, Jan. 2009.

[11] Z. Ding *et al.*, "An improved PolSAR image speckle reduction algorithm based on structural judgment and hybrid four-component polarimetric decomposition," *IEEE Trans. Geosci. Remote Sens.*, vol. 51, no. 8, pp. 4438–4449, Aug. 2013.

[12] J. Schou and H. Skriver, "Restoration of polarimetric SAR images using simulated annealing," *IEEE Trans. Geosci. Remote Sens.*, vol. 39, no. 9, pp. 2005–2016, Sep. 2001.

[13] J. Chen, Y. Chen, W. An, Y. Cui, and J. Yang, "Nonlocal filtering for polarimetric SAR data: A pretest approach," *IEEE Trans. Geosci. Remote Sens.*, vol. 49, no. 5, pp. 1744–1754, May 2011.

[14] O. D'Hondt, S. Guillaso, and O. Hellwich, "Iterative bilateral filtering of polarimetric SAR data," *IEEE J. Sel. Topics Appl. Earth Observ. Remote Sens.*, vol. 6, no. 3, pp. 1628–1639, Jun. 2013.

[15] S. Sun, J. Tian, Z. Liu, and N. Cai, "Anisotropic diffusion for speckle filtering of polarimetric synthetic aperture radar imagery," *J. Electron. Imaging*, vol. 22, no. 1, p. 013003, 2013.

[16] P. Perona and J. Malik, "Scale-space and edge detection using anisotropic diffusion," *IEEE Trans. Pattern Anal. Mach. Intell.*, vol. 12, no. 7, pp. 629–639, Jul. 1990.

[17] Y. Yu and S. T. Acton, "Speckle reducing anisotropic diffusion," *IEEE Trans. Image Process.*, vol. 11, no. 11, pp. 1260–1270, Nov. 2002.

[18] K. Krissian, C. F. Westin, R. Kikinis, and K. G. Vosburgh, "Oriented speckle reducing anisotropic diffusion," *IEEE Trans. Image Process.*, vol. 16, no. 5, pp. 1412–1424, May 2007.

[19] N. Goodman, "Statistical analysis based on a certain multivariate complex Gaussian distribution (an introduction)," *Ann. Math. Statist.*, vol. 34, no. 1, pp. 152–177, 1963.

[20] F. T. Ulaby, T. F. Haddock, and R. T. Austin, "Fluctuation statistics of millimeter wave scattering from distributed targets," *IEEE Trans. Geosci. Remote Sens.*, vol. 26, no. 3, pp. 268–281, May 1988.

[21] C. López Martinez, "*Multidimensional speckle noise. Modelling and filtering related to SAR data*," Ph.D. dissertation, Universitat Politècnica de Catalunya, Barcelona, Spain, 2003.
[22] J. Canny, "A computational approach to edge detection," *IEEE Trans. Pattern Anal. Mach. Intell.*, vol. PAMI-8, no. 6, pp. 679–698, Nov. 1986.
[23] K. Conradsen, A. A. Nielsen, J. Schou, and H. Skriver, "A test statistic in the complex Wishart distribution and its application to change detection in polarimetric SAR data," *IEEE Trans. Geosci. Remote Sens.*, vol. 41, no. 1, pp. 4–19, Jan. 2003.
[24] G. J. M. Parker and J. A. Schnabel, "Enhancement of anisotropic diffusive filtering of MR images using approximate entropy," in *Proc. 7th Annu. Meet. ISMRM*, Philadelphia, PA, USA, 1999, vol. 7, p. 175.
[25] P. Liang and Y. F. Wang, "Local scale controlled anisotropic diffusion with local noise estimate for image smoothing and edge detection," in *Proc. 6th Int. Conf. Comput. Vis.*, Bombay, India, 1998, pp. 193–200.
[26] Y. Wang, R. Niu, L. Zhang, and H. Shen, "Region-based adaptive anisotropic diffusion for image enhancement and denoising," *Opt. Eng.*, vol. 49, no. 11, pp. 117007–117007-19, 2010.
[27] J. H. Elder and S. W. Zucker, "Local scale control for edge detection and blur estimation," *IEEE Trans. Pattern Anal. Mach. Intell.*, vol. 20, no. 7, pp. 699–716, Jul. 1998.
[28] P. K. Saha and J. K. Udupa, "Scale-based diffusive image filtering preserving boundary sharpness and fine structures," *IEEE Trans. Med. Imaging*, vol. 20, no. 11, pp. 1140–1155, Nov. 2001.
[29] J. S. Lee, S. R. Cloude, K. P. Papathanassiou, M. R. Grunes, and I. H. Woodhouse, "Speckle filtering and coherence estimation of polarimetric SAR interferometry data for forest applications," *IEEE Trans. Geosci. Remote Sens.*, vol. 41, no. 10, pp. 2254–2263, Oct. 2003.
[30] Y. Yong, W. Xu, A. Tannenbaum, and M. Kaveh, "Behavioral analysis of anisotropic diffusion in image processing," *IEEE Trans. Image Process.*, vol. 5, no. 11, pp. 1539–1553, Nov. 1996.
[31] A. Freeman and S. L. Durden, "A three-component scattering model for polarimetric SAR data," *IEEE Trans. Geosci. Remote Sens.*, vol. 36, no. 3, pp. 963–973, May 1998.
[32] S. R. Cloude and E. Pottier, "An entropy based classification scheme for land applications of polarimetric SAR," *IEEE Trans. Geosci. Remote Sens.*, vol. 35, no. 1, pp. 68–78, Jan. 1997.
[33] J. J. Zyl, H. A. Zebker, and C. Elachi, "Imaging radar polarization signatures: Theory and observation," *Radio Sci.*, vol. 22, pp. 529–543, 1987.
[34] G. Vasile, J.-P. Ovarlez, F. Pascal, and C. Tison, "Coherency matrix estimation of heterogeneous clutter in high-resolution polarimetric SAR images," *IEEE Trans. Geosci. Remote Sens.*, vol. 48, no. 4, pp. 1809–1826, Apr. 2010.
[35] L. Bombrun and J.-M. Beaulieu, "Fisher distribution for texture modeling of polarimetric SAR data," *IEEE Geosci. Remote Sens. Lett.*, vol. 5, no. 3, pp. 512–516, Jul. 2008.

Xiaoshuang Ma received the B.S. degree in geographic information system from Hubei University, Wuhan, China, in 2011. He is currently pursuing the Ph.D. degree at the School of Resource and Environmental Sciences, Wuhan University, Wuhan, China.

His research interests include synthetic aperture radar image interpretation (segmentation and classification) and SAR signal processing.

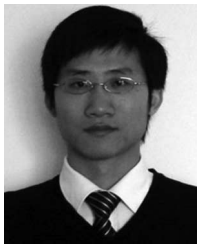

Huanfeng Shen (M'11–SM'13) received the B.S. degree in engineering of surveying and mapping and the Ph.D. degree in photogrammetry and remote sensing from Wuhan University, Wuhan, China, in 2002 and 2007, respectively.

From 2006 to 2007, he served as a Research Assistant with the Department of Mathematics, Hong Kong Baptist University, Kowloon, Hong Kong. He is currently a Professor with the School of Resource and Environmental Sciences, Wuhan University. He has published more than 60 research papers. His research interests include image processing and fusion, remote sensing application, and global change.

Liangpei Zhang (M'06–SM'08) received the B.S. degree in physics from Hunan Normal University, Changsha, China, in 1982, the M.S. degree in optics from the Xi'an Institute of Optics and Precision Mechanics, Chinese Academy of Sciences, Xi'an, China, in 1988, and the Ph.D. degree in photogrammetry and remote sensing from Wuhan University, Wuhan, China, in 1998.

He is currently with the State Key Laboratory of Information Engineering in Surveying, Mapping, and Remote Sensing, Wuhan University, as the Head of the Remote Sensing Division. He is a "Chang-Jiang Scholar" Chair Professor appointed by the Ministry of Education, China. He is currently a Principal Scientist with the China State Key Basic Research Project from 2011 to 2016 appointed by the Ministry of National Science and Technology of China to lead the remote sensing program in China. He has more than 260 research papers and five patents. He edits several conference proceedings, issues, and the Geoinformatics Symposiums. His research interests include hyperspectral remote sensing, high resolution remote sensing, image processing, and artificial intelligence.

Dr. Zhang serves as an Associate Editor of the IEEE TRANSACTIONS ON GEOSCIENCE AND REMOTE SENSING, *the International Journal of Ambient Computing and Intelligence, the International Journal of Image and Graphics, the International Journal of Digital Multimedia Broadcasting, the Journal of Geospatial Information Science, and the Journal of Remote Sensing.* He is an Executive Member (Board of Governor) of the China National Committee of International Geosphere-Biosphere Programme, Executive Member for the China Society of Image and Graphics. He regularly serves as a CoChair of the series SPIE Conferences on Multispectral Image Processing and Pattern Recognition, Conference on Asia Remote Sensing, and many other conferences.

Jie Yang received the Ph.D. degree from the Wuhan University, Wuhan, China, in 2004.

From 2011, he has held a Professor position with the State Key Laboratory of Information Engineering in Surveying, Mapping, and Remote Sensing, Wuhan University. His research interests include understanding SAR images.

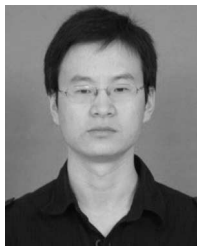

Hongyan Zhang (M'13) received the B.S. degree in geographic information system and the Ph.D. degree in photogrammetry and remote sensing from Wuhan University, Wuhan, China, in 2005 and 2010, respectively.

He is currently an Associate Professor with the State Key Laboratory of Information Engineering in Surveying, Mapping, and Remote Sensing, Wuhan University. His research interests include image reconstruction, sparse representation, and low rank methods for sensing image imagery.

Dr. Zhang is a Reviewer of several international academic journals, including IEEE TRANSACTION ON GEOSCIENCE AND REMOTE SENSING, IEEE TRANSACTION ON IMAGE PROCESSING, IEEE JOURNAL OF SELECTED TOPICS IN APPLIED EARTH OBSERVATIONS AND REMOTE SENSING, IEEE GEOSCIENCE AND REMOTE SENSING LETTERS and so on.